Effect of pyridine modification of Ni-DOBDC on CO_2 capture under humid conditions

Youn-Sang Bae,*[a] Jian Liu,[b] Christopher E. Wilmer,[c] Hahnbi Sun,[c] Allison N. Dickey,[c] Min Bum Kim,[a] Annabelle I. Benin,[d] Richard R. Willis,[d] Dushyant Barpaga,[b] M. Douglas LeVan*[b] and Randall Q. Snurr*[c]

[a] *Department of Chemical and Biomolecular Engineering, Yonsei University, 262 Seongsanno, Seodaemun-gu, Seoul 120-749, S. Korea. Tel: 82-2-2123-2755; E-mail: mowbae@yonsei.ac.kr*
[b] *Department of Chemical and Biomolecular Engineering, Vanderbilt University, PMB 351604, Nashville,Tennessee 37235-1604; E-mail: m.douglas.levan@vanderbilt.edu*
[c] *Department of Chemical & Biological Engineering, Northwestern University, 2145 Sheridan Road, Evanston, Illinois 60208-3120. Tel: 1-847-467-2977; E-mail: snurr@northwestern.edu*
[d] *UOP LLC, a Honeywell Company, Des Plaines, Illinois 60017.*

Supporting Information

1. Experimental methods

The Ni-DOBDC sample was synthesized at UOP following procedures in the literature.[1-3] Briefly, nickel acetate (18.7 g, 94.0 mmol, Aldrich) and 2,5-dihydroxyterephthalic acid (37.3 g, 150 mmol, Aldrich) were placed in 1 L of mixed solvent consisting of equal parts tetrahydrofuran (THF) and deionized water. The mixture was then put into a 2 L Parr reactor and heated at 110˚C for 3 d. The as-synthesized sample was filtered and washed with water. Then, the sample was dried in air, and the solvent remaining inside the sample was exchanged with ethanol 6 times over 8 d. Finally, the sample was heated under nitrogen and stored in a dry box for later measurements. Prior to pyridine modification or further characterization, the Ni-DOBDC was activated at 150 ^{o}C under vacuum for 12 h.

The pyridine modification procedure was adopted from the literature.[4, 5] 0.8 g of Ni-DOBDC was added to a mixed solvent composed of 48 ml chloroform and 16 ml pyridine. The mixed

solution then was stirred for 3 h and let stand for 24 h in a chemical hood to synthesize the pyridine-modified Ni-DOBDC. The as-synthesized sample was filtered and dried in the hood under ambient conditions for later use.

Powder X-ray diffraction (PXRD) patterns and the Brunauer-Emmett-Teller (BET) surface area characterization results were obtained for both unmodified and pyridine-modified Ni-DOBDC samples. BET surface areas and pore volumes were obtained using a Micromeritics ASAP 2020 porosimeter with nitrogen adsorbed at 77 K.

A volumetric system reported in our previous paper[2] was used to measure the CO_2 and H_2O adsorption equilibrium. Py-Ni-DOBDC was activated at 150 ^oC under vacuum for 12 h before isotherm measurements. The whole apparatus was put inside an environmental chamber (Thermotron SE-300) to keep experimental temperature constant. After the sample cooled down to the experimental temperature, CO_2 and water vapor were introduced into the system by flow and liquid injection, respectively. The mixtures were circulated in the closed loop by a circulation pump at a rate of about 1.0 L/min. Equilibrium was determined by using a gas chromatograph (GC, HP-6890) with a thermal conductivity detector (TCD). Calibration curves for both CO_2 and H_2O GC signals were obtained before the adsorption experiments. In a typical CO_2/H_2O binary equilibrium experiment, water was first injected into the system. After reaching equilibrium, the water loadings were constant (varied only 1.2% of their values) through the CO_2 isotherm measurement processes due to the strong interactions between the MOF structures and H_2O molecules. The sample was regenerated again using the same procedure as described above before the next isotherm measurement.

Thermogravimetric analysis (TGA) was used to estimate the amount of pyridine that was successfully incorporated into the MOF framework by examining both activated Ni-DOBDC and Py-Ni-DOBDC. A Q600 SDT Thermal Analysis instrument was used with approximately 50 mg of a sample in an aluminum cup. As purge gas, 10 mL/min of air was passed continuously across the sample during the experiment. Beginning with an equilibration at 35 ^oC, the sample was heated at a rate of 5 ^oC/min to a final temperature of 600 ^oC, which was maintained for 5 h.

2. Simulation methods

The geometrical structures of unmodified and modified Ni-DOBDC MOFs used in the simulations are presented in **Fig. S1**. The structure for dehydrated Ni-DOBDC (simply denoted as 'Ni-DOBDC' in this paper) was made by deleting all of the coordinated water molecules from the experimentally determined crystal structure of hydrated Ni-DOBDC. Since the experimentally determined crystal structure of hydrated Ni-DOBDC does not provide the exact positions of hydrogen atoms in the coordinated water molecules, a geometry optimization was performed to find proper positions of the hydrogen atoms using a cluster model. In this DFT calculation, the Gaussian 09 software[6] was used at the B3LYP level of theory with a basis set of 6-31+G(d,p). Then, the structure for hydrated Ni-DOBDC (denoted as 'hy-Ni-DOBDC' in this paper) was made by replacing all of the metal sites with those from the optimized cluster using software called 'FunctionalizeThis' written by our group. 'FunctionalizeThis' automates the process of altering a repeating motif in a large molecule or periodic structure, avoiding the need to do it by hand. See Section 3 for details. In order to make pyridine-modified Ni-DOBDC structures, a geometry optimization was again performed to find proper positions of the pyridine atoms using a cluster model. Again, Gaussian 09[6] was used at the B3LYP level of theory with a basis set of 6-31+G(d,p). Then, the structures for pyridine-modified hy-Ni-DOBDC were made

by replacing some portion of the coordinated water molecules with the appropriate atoms from the optimized cluster using the 'FunctionalizeThis' software. 16%Py-hy-Ni-DOBDC, 33%Py-hy-Ni-DOBDC, and 50%Py-hy-Ni-DOBDC were made by replacing one, two, and three of the six corners in the hexagonal channels with the optimized pyridine molecule, respectively. Three types of 33%Py-hy-Ni-DOBDC (33%Py-a, 33%Py-b, and 33%Py-c) were created depending on the positions of the two pyridines in the hexagonal channel (**Fig. S1**). For 50%Py-hy-Ni-DOBDC, the pyridine molecules are assumed to be located at every other corner in the hexagonal channel.

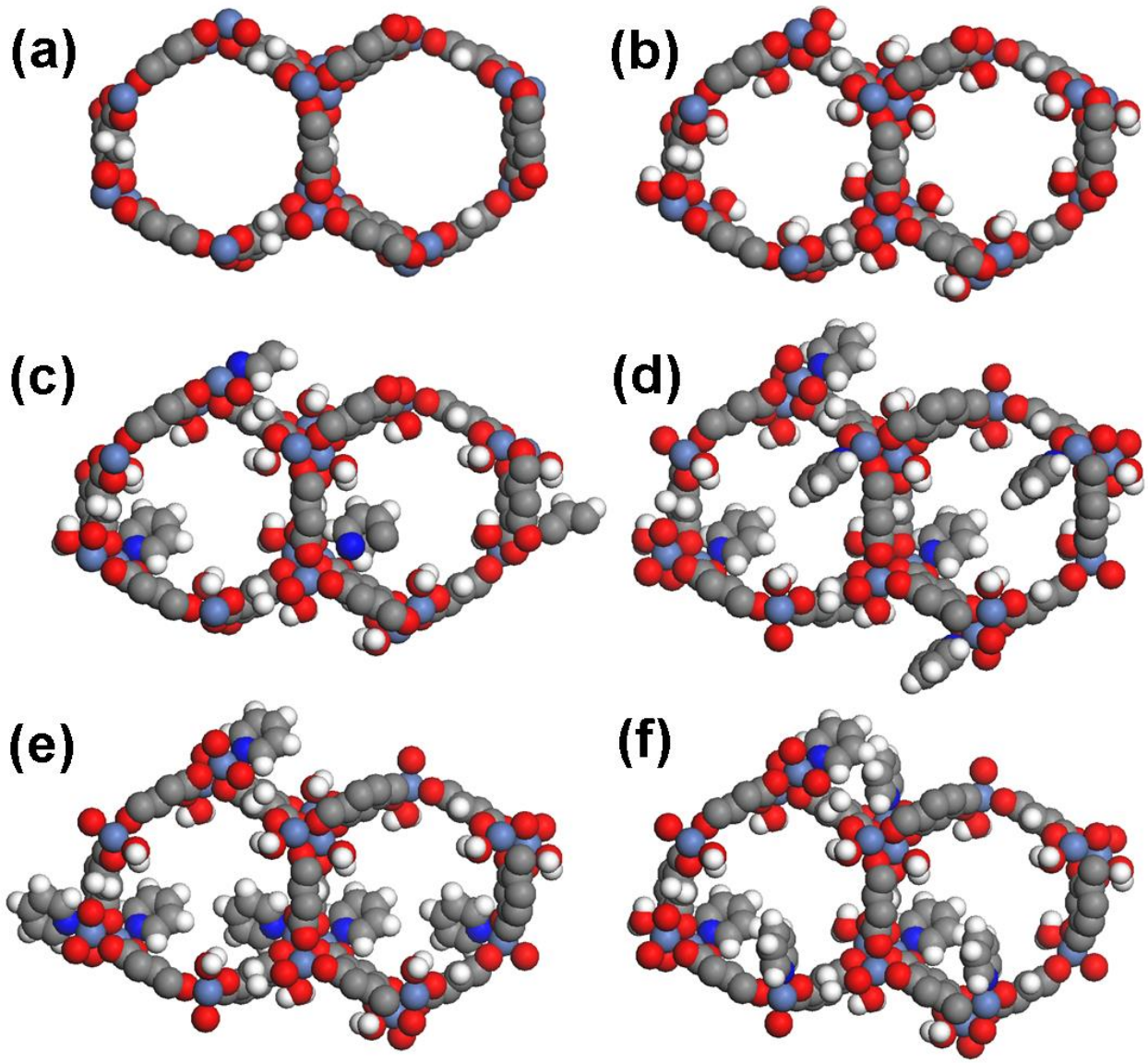

Fig. S1. Geometrical structures of unmodified and modified MOFs: (a) Ni-DOBDC, (b) hy-Ni-DOBDC, (c) 16%Py-hy-Ni-DOBDC, (d) 33%Py-a-hy-Ni-DOBDC, (e) 33%Py-b-hy-Ni-DOBDC, and (f) 33%Py-c-hy-Ni-DOBDC.

Several different water models including TIP3P,[7] TIP4P,[7] TIP4P-Ew,[8] TIP5P-Ew,[9] SPC,[10] and SPC/E[11] were tested to see if they reproduced the experimental phase diagram of bulk water in the density-temperature plane[12] (**Fig. S2**). Among these models, TIP4P-Ew and SPC/E were found to reproduce the experimental data well. Since TIP4P-Ew is more computationally expensive than SPC/E, the SPC/E model was used in this study. Partial charges and Lennard-Jones parameters for CO_2 were taken from the TraPPE force field,[13] which models the CO_2 molecule as a rigid and linear structure with a partial charge of $-0.35e$ on the O atoms and a partial charge of $+0.70e$ on the C atom.

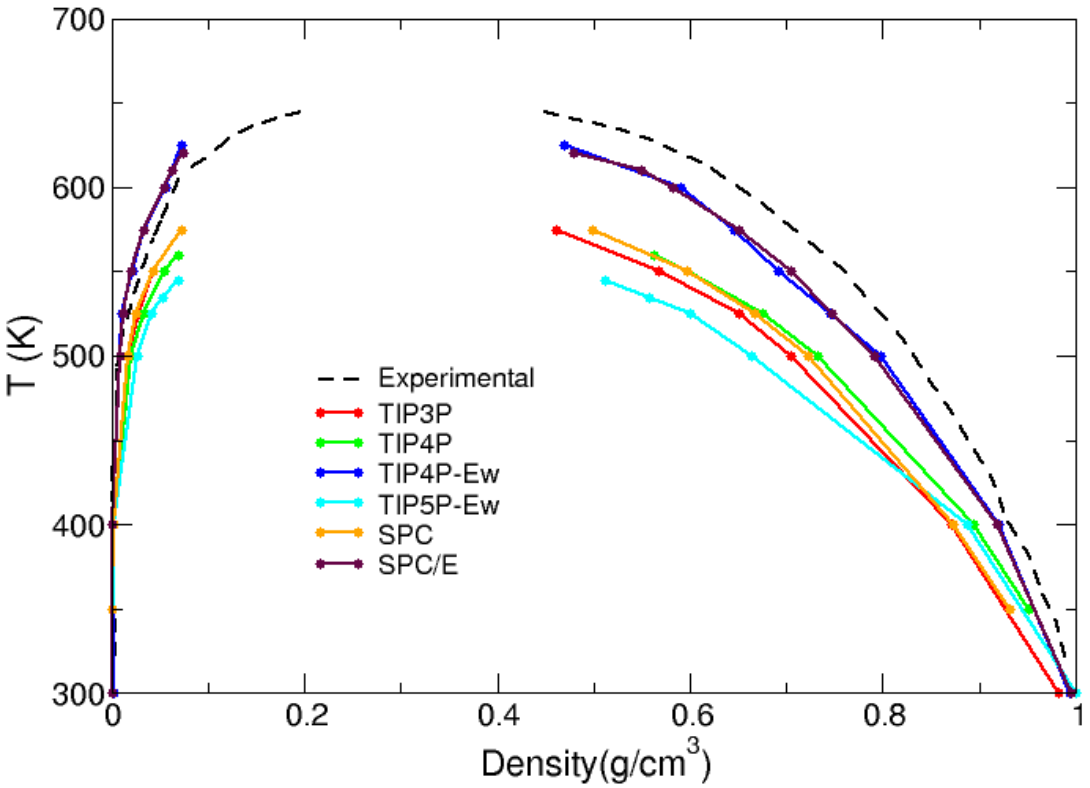

Fig. S2. Comparison of the experimental and simulated VLE curves for bulk water using various water models.

Framework atoms (including pyridine) were considered fixed at their crystallographic coordinates and modelled with Lennard-Jones parameters from the DREIDING force field[14], except for the nickel atom which is not available in DREIDING and in which case we used values from the Universal Force Field.[15] Lorentz-Berthelot mixing rules were used for the gas/framework and gas/gas interactions. The partial charges of framework atoms were calculated using representative fragments of the framework, using the CHELPG method provided in the program Gaussian09 following DFT calculations with the B3LYP density functional and a 6-31G* basis set. Representative fragments contained either pyridine or water

molecules coordinated to the open-metal sites, but not both simultaneously. Hence, to determine partial charges of frameworks containing both pyridines and coordinated water molecules, a distance-weighted averaging scheme was used so that the closer an atom is to a pyridine or water molecule, the closer its partial charge is to the value in the corresponding representative fragment. See Section 4 for details. A Lennard-Jones cutoff of 12 Å was used, and all charge interactions were calculated with Ewald summation.

The GCMC simulations were performed with the RASPA code[16] to calculate single-component isotherms of CO_2 and H_2O. Translation, rotation, insertion, and deletion moves of gas molecules were used during the simulations. All data reported are excess adsorption isotherms, which can be calculated using absolute adsorption values, the pore volume, and the bulk fluid density.[17] 1×10^6 moves were used for each equilibration and 1×10^6 moves were used for calculating ensemble averages.

The accessible surface area and total pore volume of each structure was calculated in a geometric fashion using a simple Monte Carlo integration technique.[18, 19] Nitrogen-sized (3.72 Å) and zero-sized (0 Å) probes were used for the calculations of the accessible surface area and the total pore volume, respectively. In these calculations, the van der Waals diameters of framework atoms were used, and these were taken from the DREIDING force field[14], except for the nickel atom which is not available in DREIDING and which was found in UFF.[15]

3. FunctionalizeThis software

We wrote the software 'FunctionalizeThis' to alter repeating motifs in large molecules or periodic systems in an automated way. The software can concisely be described as a 'search-and-replace' tool for molecular structures. There are three inputs: 1) a molecular system, 2) a molecular pattern to search for, and 3) a molecular pattern to replace the prior one, hereafter called a "functional group." The only output is the new molecular system. **Fig. S3** illustrates the idea.

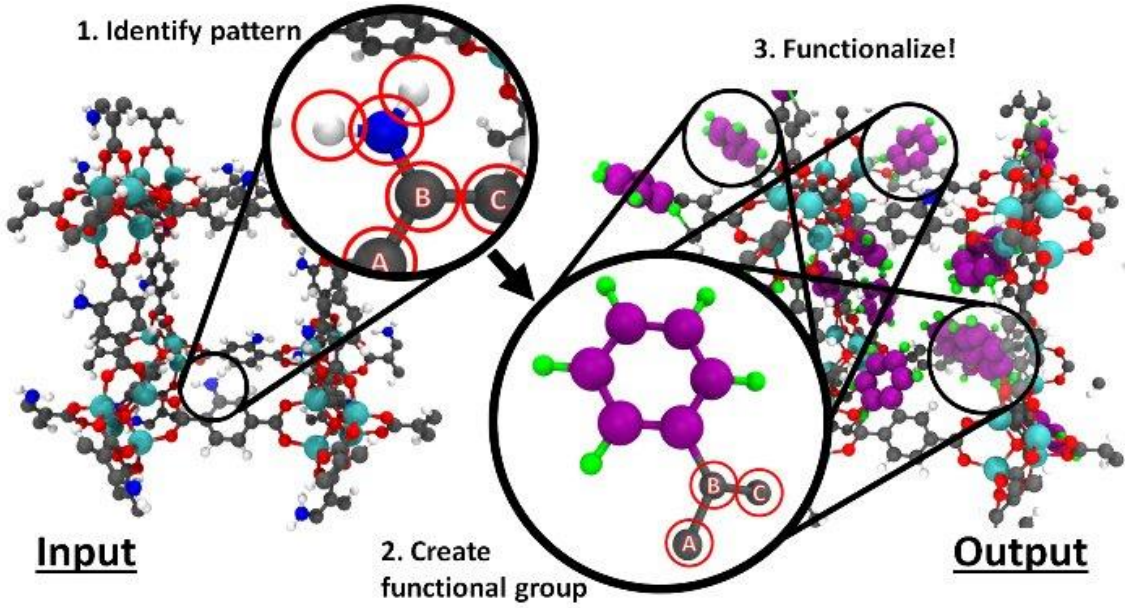

Fig. S3. A schematic illustrating the conceptual function of the 'FunctionalizeThis' software.

Pattern files are created by choosing a subset of atoms in the original system and then choosing three atoms to be "primary", "secondary" and "tertiary" for orientation purposes (see sample file in **Fig. S4** below). The program will "match" the pattern in other parts of the molecule by comparing distances and atom types between atoms in the pattern and candidate atoms elsewhere. This requires that patterns are chosen such that the distances between atoms are all different. See **Fig. S5**.

```
irmof3patternA

  created with ArgusLab version 4.0.1
  6  0  0  0  0  0  0  0  0  0  0 V2000
   -1.1531    1.5305    0.4742 C   0  0  0  0  0  0  0  0  0  0  0  0 secondary
   -2.5507    1.5695    0.3967 C   0  0  0  0  0  0  0  0  0  0  0  0 primary
   -3.2878    0.7511    1.2877 C   0  0  0  0  0  0  0  0  0  0  0  0 tertiary
   -3.1417    2.3705   -0.5063 N   0  0  0  0  0  0  0  0  0  0  0  0 none
   -2.5797    2.9305   -1.1299 H   0  0  0  0  0  0  0  0  0  0  0  0 none
   -4.1609    2.3849   -0.5224 H   0  0  0  0  0  0  0  0  0  0  0  0 none
M  END
```

Fig. S4. Sample pattern file in the MOL format.

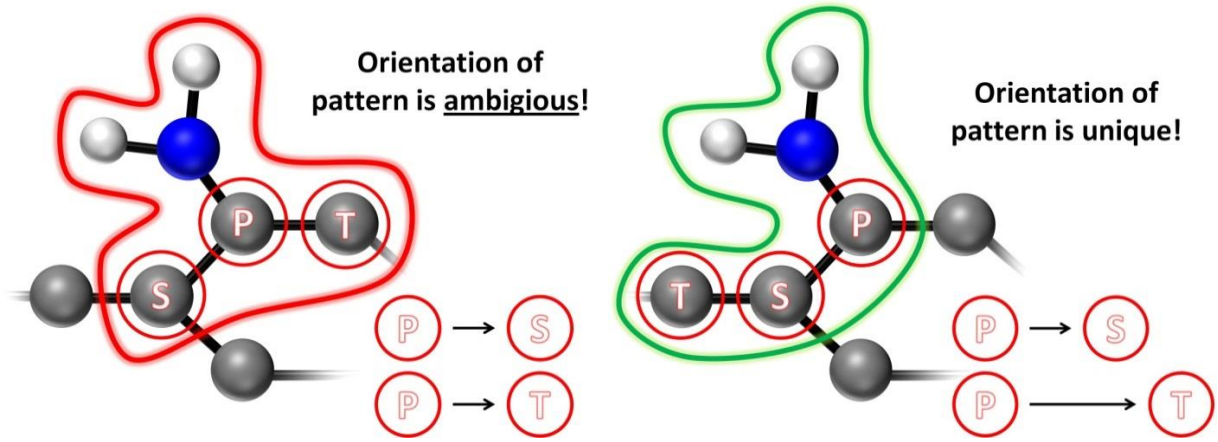

Fig. S5. Patterns in the molecular system are identified based on matching distances between atoms in the pattern file and in the system. Therefore, it is better to choose patterns where the distances between atoms are unique.

4. Determining partial charges

Partial charges for the pyridine-functionalized Ni-DOBDC framework were determined in three steps. First, quantum chemistry techniques were applied to fragments of the Ni-DOBDC framework to obtain the electrostatic potential using the B3LYP density functional and a 6-31G* basis set. Partial charges were assigned to these fragments by the fitting to reproduce the electrostatic potentials using the ChelpG method provided in the program Gaussian09. Charges were obtained in this way for fragments with water-coordinated Ni sites and separately for fragments with pyridine-functionalized Ni sites. Second, the 'FunctionalizeThis' program was used to distribute pyridines in a controlled way in the Ni-DOBDC framework (replacing coordinated water molecules at corresponding Ni sites). Third, depending on whether an atom was closer to a water-coordinated Ni site or a pyridine-functionalized Ni site, its partial charge was assigned to more closely resemble that of the equivalent atom in the corresponding fragment. The details of this assignment are outlined below.

Let T be the total number of atoms in a repeating unit cell, which depends on the ratio of water-coordinated sites, W, to pyridine-functionalized sites, P. Let N be the number of atoms in the unit cell not counting those of the water and pyridine molecules (thus N is independent of the ratio of W to P). From ChelpG calculations, we have two overlapping sets of charges for the T atoms in the unit cell: one set of charges are for the water molecules and N framework atoms, and the other set of charges are for the pyridines and N framework atoms. We are now concerned with how to combine the charges for the N atoms that have two sets to choose from. The partial charge, Q, on the i^{th} atom is given by:

$$Q_i = A_i Q_{iW} + B_i Q_{iP}$$

where A_i and B_i are the weighting coefficients (to be determined later) and Q_{iW} and Q_{iP} are the partial charges of an atom in the water-coordinated Ni site fragment and the pyridine-functionalized fragment respectively.

In a unit cell where some of the Ni sites are functionalized with pyridines and some are coordinated with water molecules, the weighting coefficients are determined by the proximity of an atom to these Ni sites. Specifically,

$$A_i = \frac{1}{K}\sum_{j=1}^{M_W}\frac{1}{|r_i - r_{jW}|^2}, \qquad B_i = \frac{1}{K}\sum_{j=1}^{M_P}\frac{1}{|r_i - r_{jP}|^2}$$

where r_i is the position vector of the i^{th} atom, r_{jW} and r_{jP} are the position vector of water-coordinated Ni sites and the position vector of pyridine-functionalized Ni sites, respectively, K is a normalization constant such that $A_i + B_i = 1$, and M_W and M_P are the number of water-coordinated Ni sites and the number of pyridine-functionalized Ni sites, respectively.

Charges obtained the way described above are not guaranteed to result in a charge neutral framework, but the excess charge is expected to be small, since each fragment is charge neutral. To account for this, we shifted the charge of every atom in the system uniformly by a small amount to ensure charge neutrality.

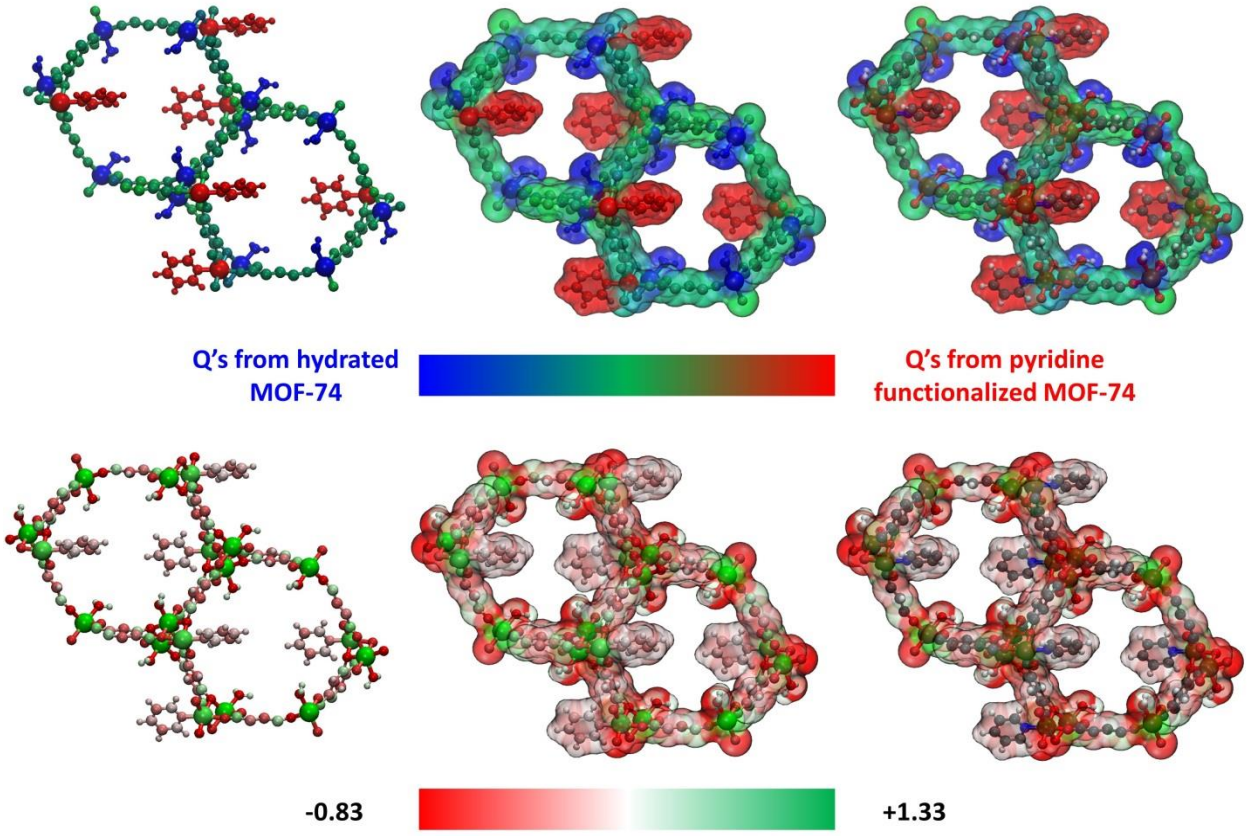

Fig. S6. An example of partial charge determination for 33%Py-a-hy-Ni-DOBDC. The top row shows atoms colored according to the weighting coefficients (blue corresponds to atoms with partial charges most closely resembling the water-coordinated fragment, red corresponds to atoms with partial charges most closely resembling the pyridine-functionalized fragment). The bottom row shows atoms colored according to their resulting partial charges. In both the top and bottom rows, the same data are depicted in three different styles to aide in visualizing the information (the transparent surface in the middle and right columns is strictly a visual aide and does not represent any physical quantity).

5. Additional adsorption data and discussion

Table S1. BET surface areas and total pore volumes of experimental samples

	BET surface area [$m^2 g^{-1}$]	Total pore volume [$cm^3 g^{-1}$]
Ni-DOBDC	798	0.38
Py-Ni-DOBDC	409	0.18

Table S2. Calculated accessible surface areas and total pore volumes of MOF models

	Acc. surface area [$m^2 g^{-1}$]*	Total pore volume [$cm^3 g^{-1}$]**
Ni-DOBDC	1182	0.60
hy-Ni-DOBDC	796	0.35
16%Py-hy-Ni-DOBDC	593	0.28
33%Py-a-hy-Ni-DOBDC	156	0.20
33%Py-b-hy-Ni-DOBDC	231	0.21
33%Py-c-hy-Ni-DOBDC	433	0.23

*Accessible surface areas were calculated using a nitrogen probe.

**Total pore volumes were calculated from a GCMC simulation for helium adsorption at 298 K.

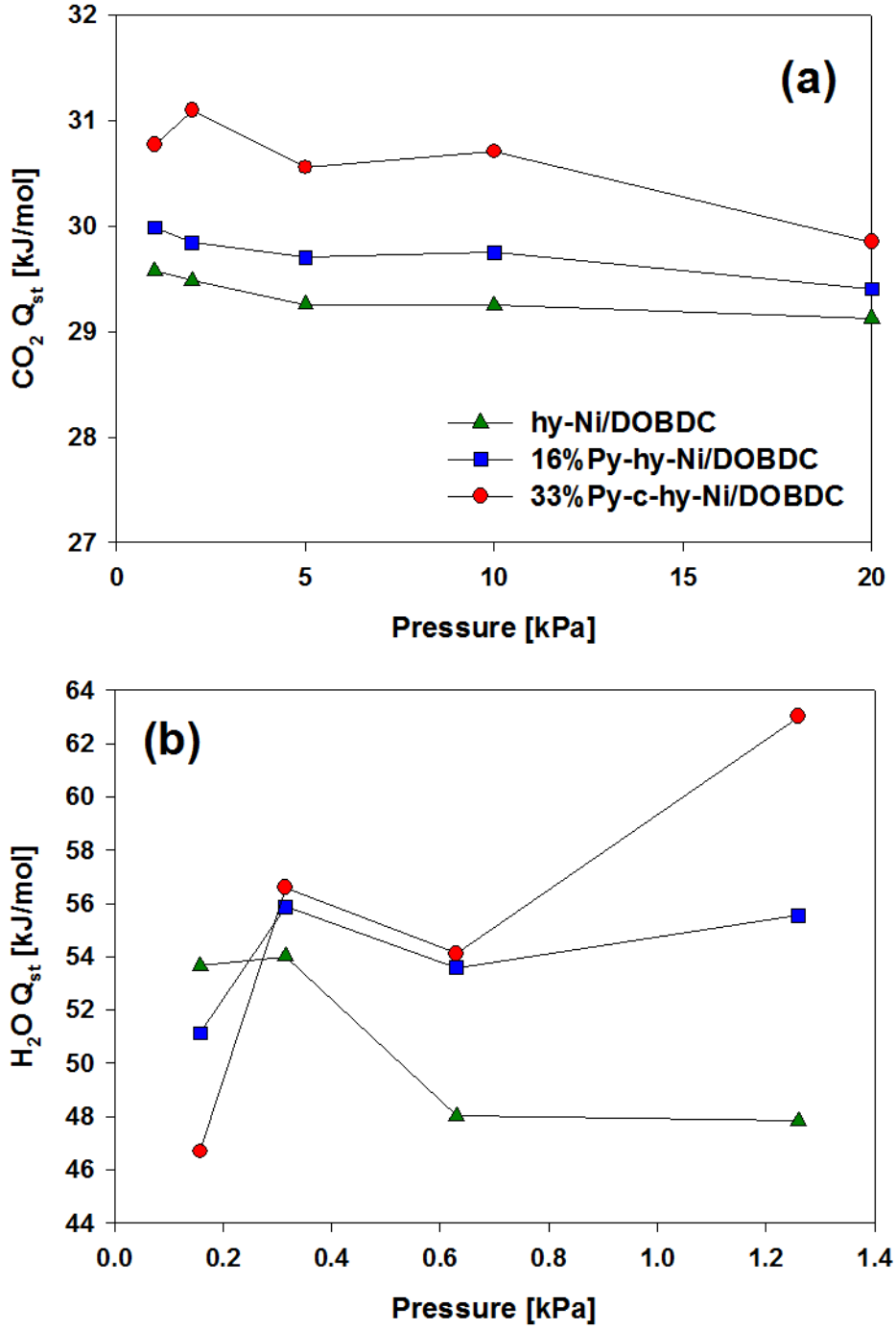

Fig. S7. Calculated Q_{st} from GCMC simulations for (a) CO_2 and (b) H_2O in unmodified and pyridine-modified Ni-DOBDC materials.

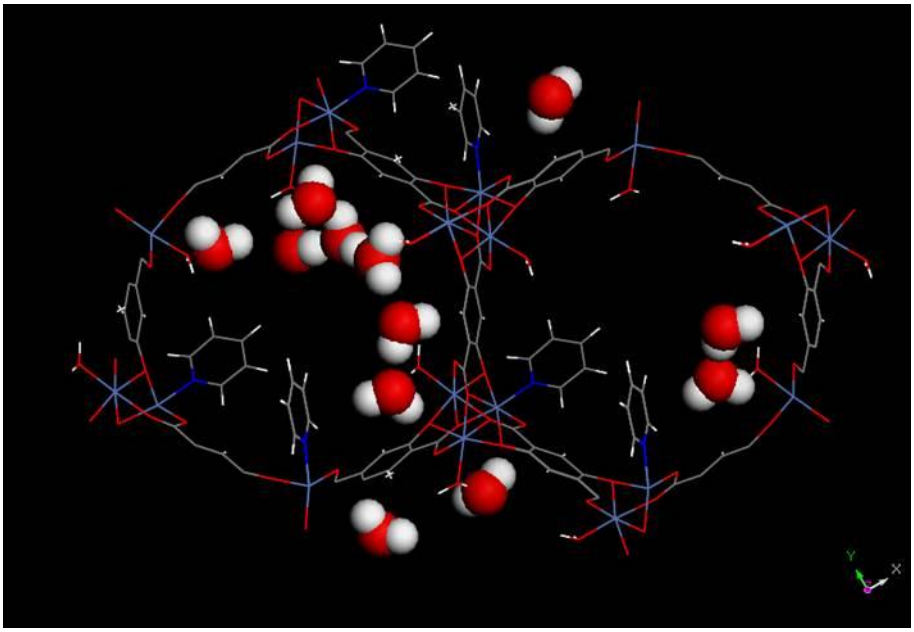

Fig. S8. A snapshot of H_2O adsorption in 33%Py-c-hy-Ni-DOBDC at 157 Pa.

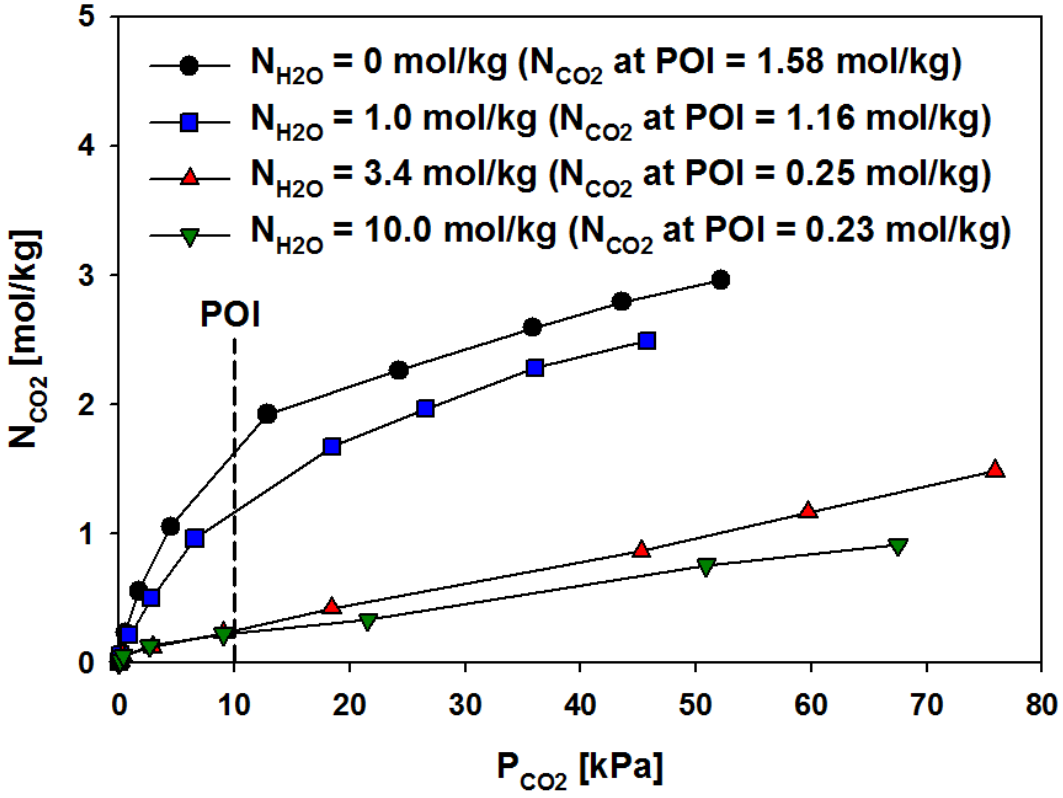

Fig. S9. Experimental CO_2 isotherms at 298 K for Py-Ni-DOBDC with different amounts of preloaded H_2O.

Table S3. Comparison of H_2O/CO_2 selectivities[a)] at 45% RH conditions (P_{H2O}=1.41 kPa) and the POI (P_{CO2}=10 kPa) between Ni-DOBDC and Py-Ni-DOBDC

	Ni-DOBDC	Py-Ni-DOBDC
H_2O uptake (mol/kg)	26	10
CO_2 uptake (mol/kg)	0.10	0.23
H_2O/CO_2 selectivity (-)	1844	308

[a)] H_2O/CO_2 selectivity = $S_{H2O/CO2} = (N_{H2O}/N_{CO2})/(y_{H2O}/y_{CO2})$. Here, N is the adsorbed amount and y is the mole fraction in the gas phase.

6. TGA and pyridine loading

The pyridine loading for the Ni-DOBDC after activation was determined experimentally using thermogravimetric analysis (TGA). Results are shown in Figure S10 for Ni-DOBDC and Py-Ni-DOBDC. We made two assumptions in analyzing the TGA weight loss data in order to estimate the pyridine loading. First, we assumed that water and solvent molecules were removed by 170 ^{o}C, a temperature at which the Py-Ni-DOBDC curve had an inflection point, and this was used as the starting point of the analysis. Second, we assumed that any decomposition of pyridine left no residue. Thus, the difference between the curves in Figure S10 is attributed to pyridine. Then, based on the weight loss data, the pyridine loading could be determined by material balance on a water-free and solvent-free basis. Based on weights at 600 ^{o}C, the pyridine loading after activation was 0.115 g pyridine per g Ni-DOBDC or 10.3 wt%. We note that if decomposition were complete at 350 ^{o}C, then the pyridine loading would be 0.163 g pyridine per g Ni-DOBDC or 14.0 wt%. Given that any pyridine lost before 170 ^{o}C would add to the loading, a reasonable estimate of the pyridine loading on the Ni-DOBDC is 12 ± 2 wt%.

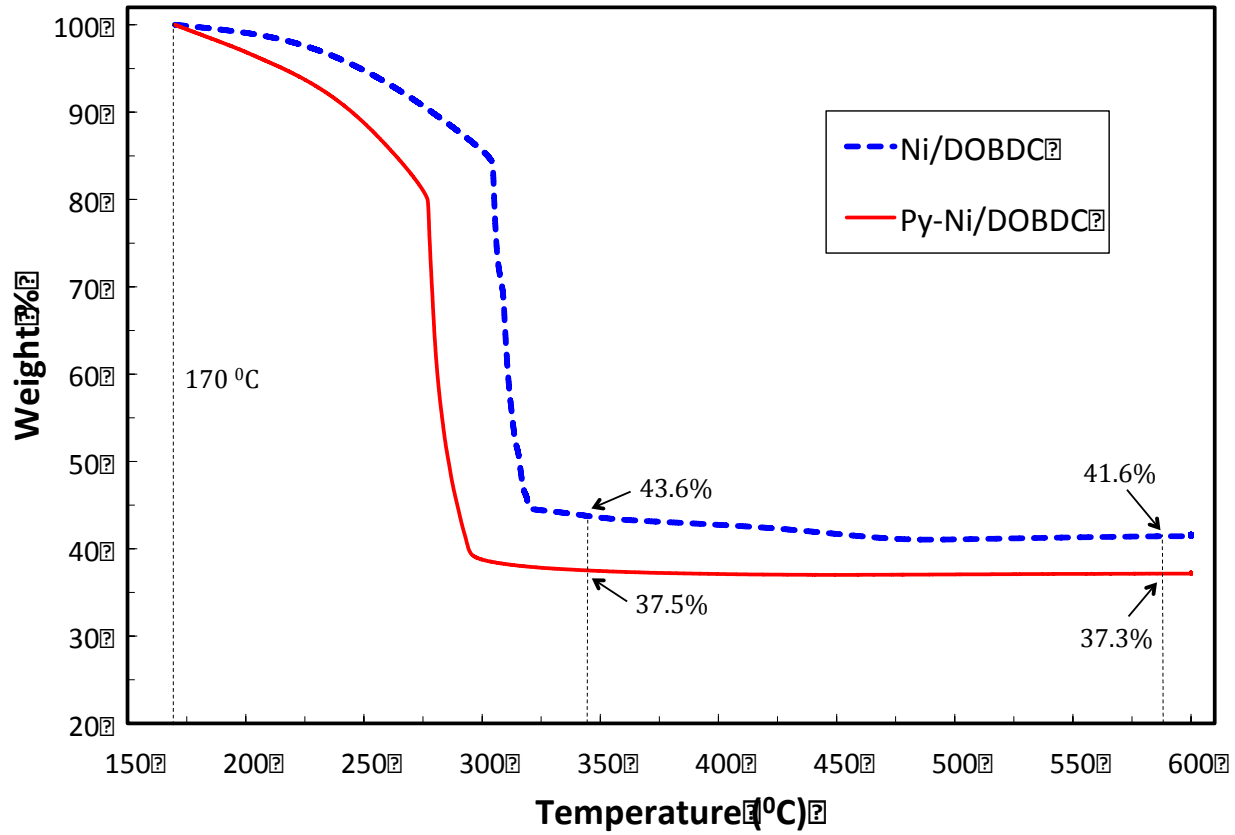

Fig. S10. TGA curves for the Ni-DOBDC samples with and without pyridine. Weight loss vs. program temperature.

References

1. S. R. Caskey, A. G. Wong-Foy and A. J. Matzger, *J. Am. Chem. Soc.*, 2008, **130**, 10870.
2. J. Liu, Y. Wang, A. I. Benin, P. Jakubczak, R. R. Willis and M. D. LeVan, *Langmuir*, 2010, **26**, 14301.
3. P. D. C. Dietzel, B. Panella, M. Hirscher, R. Blom and H. Fjellvag, *Chem. Commun.*, 2006, 959.
4. O. K. Farha, K. L. Mulfort and J. T. Hupp, *Inorganic Chemistry*, 2008, **47**, 10223.
5. Y.-S. Bae, O. K. Farha, J. T. Hupp and R. Q. Snurr, *J. Mater. Chem.*, 2009, **19**, 2131.
6. R. **A.** Gaussian 09, Frisch, M. J.; Trucks, G. W.; Schlegel, H. B.; Scuseria, G. E.; Robb, M. A.; Cheeseman, J. R.; Scalmani, G.; Barone, V.; Mennucci, B.; Petersson, G. A.; Nakatsuji, H.; Caricato, M.; Li, X.; Hratchian, H. P.; Izmaylov, A. F.; Bloino, J.; Zheng, G.; Sonnenberg, J. L.; Hada, M.; Ehara, M.; Toyota, K.; Fukuda, R.; Hasegawa, J.; Ishida, M.; Nakajima, T.; Honda, Y.; Kitao, O.; Nakai, H.; Vreven, T.; Montgomery, Jr., J. A.; Peralta, J. E.; Ogliaro, F.; Bearpark, M.; Heyd, J. J.; Brothers, E.; Kudin, K. N.; Staroverov, V. N.; Kobayashi, R.; Normand, J.; Raghavachari, K.; Rendell, A.; Burant, J. C.; Iyengar, S. S.; Tomasi, J.; Cossi, M.; Rega, N.; Millam, N. J.; Klene, M.; Knox, J. E.; Cross, J. B.; Bakken, V.; Adamo, C.; Jaramillo, J.; Gomperts, R.; Stratmann, R. E.; Yazyev, O.; Austin, A. J.; Cammi, R.; Pomelli, C.; Ochterski, J. W.; Martin, R. L.; Morokuma, K.; Zakrzewski, V. G.; Voth, G. A.; Salvador, P.; Dannenberg, J. J.; Dapprich, S.; Daniels, A. D.; Farkas, Ö .; Foresman, J. B.; Ortiz, J. V.; Cioslowski, J.; Fox, D. J. Gaussian, Inc., Wallingford CT, 2009.
7. W. L. Jorgensen, J. Chandrasekhar, J. D. Madura, R. W. Impey and M. L. Klein, *Journal of Chemical Physics*, 1983, **79**, 926.
8. H. W. Horn, W. C. Swope, J. W. Pitera, J. D. Madura, T. J. Dick, G. L. Hura and T. Head-Gordon, *Journal of Chemical Physics*, 2004, **120**, 9665.
9. S. W. Rick, *Journal of Chemical Physics*, 2004, **120**, 6085.
10. H. J. C. Berendsen, J. P. M. Postma, W. F. van Gunsteren and J. Hermans, in *Intermolecular Forces*, ed. B. Pullman, Reidel, Dordrecht, 1981.
11. H. J. C. Berendsen, J. R. Grigera and T. P. Straatsma, *Journal of Physical Chemistry*, 1987, **91**, 6269.
12. C. Vega, J. L. F. Abascal and I. Nezbeda, *Journal of Chemical Physics*, 2006, **125**, 034503.
13. J. J. Potoff and J. I. Siepmann, *AIChE J.*, 2001, **47**, 1676.
14. S. L. Mayo, B. D. Olafson and W. A. Goddard, *J. Phys. Chem.*, 1990, **94**, 8897.
15. A. K. Rappe, C. J. Casewit, K. S. Colwell, W. A. Goddard and W. M. Skiff, *J. Am. Chem. Soc.*, 1992, **114**, 10024.
16. D. Dubbeldam, S. Calero, D. E. Ellis and R. Q. Snurr, *RASPA 1.0*, (2008) Northwestern University: Evanston, IL.
17. A. L. Myers and P. A. Monson, *Langmuir*, 2002, **18**, 10261.
18. Y.-S. Bae, D. Dubbeldam, A. Nelson, K. S. Walton, J. T. Hupp and R. Q. Snurr, *Chemistry of Materials*, 2009, **21**, 4768.
19. Y.-S. Bae, A. O. Yazaydin and R. Q. Snurr, *Langmuir*, 2010, **26**, 5475.